Ecotoxicology and Environmental Safety 286 (2024) 117131

Contents lists available at ScienceDirect

Ecotoxicology and Environmental Safety

journal homepage: www.elsevier.com/locate/ecoenv

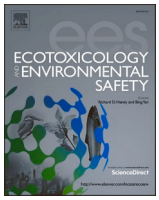

Size-dependent toxic interaction between polystyrene beads and mercury on the mercury accumulation and multixenobiotic resistance (MXR) of brackish water flea *Diaphanosoma celebensis*

Je-Won Yoo [a], Youn-Ha Lee [a], Jihee Kim [b], Seunghee Han [b], Kyun-Woo Lee [c], Young-Mi Lee [a,*]

[a] Department of Biotechnology, College of Convergence Engineering, Sangmyung University, Seoul 03016, Republic of Korea
[b] School of Earth Sciences and Environmental Engineering, Gwangju Institute of Science and Technology (GIST), Gwangju 61005, Republic of Korea
[c] Marine Biotechnology & Bioresource Research Department, Korea Institute of Ocean Science and Technology, Busan 49111, Republic of Korea

ARTICLE INFO

Keywords:
Brackish water flea
Combined toxicity
Mercury
Multixenobiotic resistance
Polystyrene beads

ABSTRACT

Due to their worldwide distribution and persistence, mercury (Hg), and nano- and microplastics (NMPs) pose major threats to global ocean ecosystems. Hg and NMPs co-exist in the ocean and can interact with each other. However, information on the toxicity of this interaction to marine biota remains limited. Thus, we investigated the toxicological interaction between $HgCl_2$ (Hg) and NMPs by studying the influence of different sizes of polystyrene beads (0.05-, 0.5-, and 6-μm) on Hg accumulation in the brackish water flea *Diaphanosoma celebensis*. The Hg adsorption capacity of NPs (0.05-μm) was higher than that of MPs (0.5- and 6-μm). Only the group co-exposed to both Hg and NPs showed increased Hg content in *D. celebensis*. Multixenobiotic resistance (MXR) activity and transcriptional modulation of transporter genes (*ABCBs* and *ABCCs*) were decreased by NMP exposure, particularly by NPs, suggesting MXR disruption by NPs. However, only the activity of multidrug resistance-associated proteins (MRPs; ABCCs) increased with Hg exposure and decreased upon NP+Hg co-exposure, indicating an important role of ABCC in Hg efflux. Furthermore, *in vivo* toxicity tests showed a synergistic toxic interaction between Hg and NPs on the reproduction of *D. celebensis*. Our findings suggest that NPs have the potential to enhance the toxicity of Hg, increasing Hg accumulation not only by serving Hg as a carrier but also by disrupting MXR.

1. Introduction

Plastic pollution is considered one of the most pressing environmental problems because plastics possess a long half-life and are ubiquitous in the environment (Ajith et al., 2020). The marine environment is particularly vulnerable to plastics pollution, serving as the final sink of plastic debris, in which plastics can be further decomposed to smaller sized particles such as microplastics (MPs; < 5 mm) and nanoplastics (NPs; < 0.1 μm) by physical factors and the microbiome (Birch et al., 2020). These nano- and microplastics (NMPs) can be consumed by marine organisms, including small zooplankton, which results in deleterious effects, such as tissue damage, metabolic disorders, reproductive disorders, and oxidative stress (Barboza et al., 2018; Cho et al., 2022; Jeon et al., 2023; Sikdokur et al., 2020). In addition to being toxic to marine organisms, NMPs also act as vectors for transferring ambient contaminants to organisms because of their high surface adsorption capacity and surface/volume ratio (Amelia et al., 2021; Brennecke et al., 2016). However, even though NMPs commonly co-exist with various pollutants in the ocean, studies on the combined toxicity of NMPs and other pollutants are still limited compared to studies on the toxicity of each as a single substrate. Thus, to better understand the potential toxicity of NMPs in marine environments, more studies on the combined toxicity of NMPs and other pollutants are required.

Mercury (Hg) is considered one of the most hazardous marine pollutants together with NMPs due to their high concentration in marine environments (average of 1.5 pM in the worldwide ocean, and ~27,060 ng/L in the contaminated region; reviewed by Gworek et al., 2016), high bioaccumulation rate (Yan et al., 2019), and toxicity such as immunotoxicity, metabolic disorders, or oxidative stress on marine organisms (Sikdokur et al., 2020; Yoo et al., 2022, 2023). Previous studies have reported that NMP co-exposure can affect Hg accumulation and toxicity in aquatic organisms; however, the results of their toxicological

* Corresponding author.
E-mail address: ymlee70@smu.ac.kr (Y.-M. Lee).

https://doi.org/10.1016/j.ecoenv.2024.117131
Received 7 February 2024; Received in revised form 9 May 2024; Accepted 26 September 2024
Available online 15 October 2024

interactions are controversial. For example, exposure of the marine copepod *Tigriopus japonicus* to a mixture of NP beads (0.05-μm; 23 μg/L) and $HgCl_2$ (1 μg/L of Hg) resulted in higher Hg accumulation and reproductive toxicity than when the copepod was exposed to Hg alone, which suggests a synergistic interaction between Hg and NPs (Xie et al., 2023). On the contrary, co-exposure of polyethylene MP beads (1–5-μm; 0.13 mg/L) induced a reduction of Hg accumulation and Hg-induced filtration disorders, metabolic disorders, neurotoxicity, and oxidative stress in the bivalve *Corbicula fluminea* (Oliveira et al., 2018). Sikdokur et al. (2020) also reported a slight decrease in Hg accumulation in the Manila clam *Ruditapes philippinarum* co-exposed to $HgCl_2$ (10 μg/L of Hg) and MPs (10–45-μm; 25 μg/L). However, the difference was not statistically significant. These different toxicological interactions may be due to experimental conditions, such as test organisms and exposure duration, but may also be due to differences in the size of MPs, given that the size of plastics is an important factor in the adsorption of contaminants and their toxicity (Jeong et al., 2018; Qiao et al., 2019). Thus, studies on the combined toxicity of Hg and NMPs, depending on the size of the NMPs, are required to better understand their toxicological interactions.

ATP-binding cassette (ABC) transporters are highly conserved in eukaryotes and are one of the largest families of transporters that use ATP to transport many endogenous and xenobiotic substrates in biota. They are classified into different subfamilies based on their structure and function: A, B, C, D, E, F, and G (El-Awady et al., 2017; Vasiliou et al., 2009). Among these, P-glycoprotein (P-gp; included in the ABCB subfamily), multidrug resistance protein (MRP; included in the ABCC subfamily), and breast cancer resistance protein (BCRP; included in the ABCG subfamily) play an important role in the efflux of xenobiotics. Thus, multi-xenobiotic resistance (MXR) driven by P-gp, MRP, and/or BCRP is considered one of the major defense systems in response to various pollutants including Hg in biota (Bridges and Zalups., 2017; Vasiliou et al., 2009).

The brackish water flea *Diaphanosoma celebensis* is a primary consumer that plays an important role in the energy transfer from primary producers to higher trophic levels in marine environments and has various advantages in laboratory-based ecotoxicological studies, including a short life cycle, small size, and high sensitivity to contaminants. In addition, the non-selective feeding strategy of water fleas, including *Diaphanosoma* spp., makes them suitable test organisms for evaluating the toxicity of particles, including NMPs (DeMott, 1986).

This study aimed to investigate the size-dependent toxic interactions of NMPs with Hg. Thus, we first analyzed Hg adsorption on three different sizes of NMPs after incubation and the accumulation of Hg in *D. celebensis* after single and combined exposure to Hg and NMPs. Subsequently, multixenobiotic resistance assay and transcriptional modulation of ABC transporter-coding genes, including P-gp (*ABCBs*) and MRP (*ABCCs*), were performed, to elucidate the single and combined effects of Hg and NMPs on MXR. This study provides a better understanding of the toxicological interactions between Hg and NMPs in marine zooplankton.

2. Materials and methods

2.1. Chemicals and test organism maintenance

Polystyrene (PS) beads were chosen as the model plastic for this study because PS is one of the most produced polymers (5.2 % of total global plastics production in 2022; PlasticsEurope, 2023) and a common polymer type of MPs in the marine environment (Cai et al., 2018; Eo et al., 2018). In particular, PS beads are the most studied NMP in ecotoxicological studies due to their experimental advantages, including ease of synthesis into various sizes and shapes (Bhagat et al., 2021; Kik et al., 2020). Three different sizes of PS beads (0.05-, 0.5-, and 6-μm in diameter) were used because these sizes include nano- to micro-sizes, and *D. celebensis* can readily ingest these sizes of MPs (Yoo et al., 2021). Non-functionalized PS beads of different sizes were purchased from Polysciences (Warrington, PA, USA) and their characterization was confirmed in our previous study (Figure S1 and Table S1; Yoo et al., 2021). Mercury (II) chloride powder ($HgCl_2$, purity $\geq$ 99.5 %) was purchased from Sigma-Aldrich (St. Louis, MO, USA), and Hg stock solution (1 g/L) was made by dissolving Hg powder in distilled water. The actual Hg ion concentrations in the Hg and NMPs stock solutions were determined using atomic absorption spectroscopy (DMA-80, Milestone, BG, Italy), as described in the EPA Method 7473 (> 80 % of the nominal concentration in the Hg stock solution and no Hg ions in the NMPs stock solution). Rhodamine B ($C_{28}H_{31}ClN_2O_3$, purity $\geq$ 95.0 %, Sigma-Aldrich) and calcein AM ($C_{46}H_{46}N_2O_{23}$, purity $\geq$ 95.0 %, Sigma-Aldrich) were used as substrates for P-gp and MRP, respectively. The brackish water flea *D. celebensis* was maintained in artificial seawater (ASW; Instant Ocean, Aquarium Systems, Sarrebourg, France) with a salinity of 15 psu at the Molecular Toxicology Laboratory of Sangmyung University (Seoul, South Korea). A photoperiod of 12 h:12 h light/dark and a temperature of 25±1°C were maintained. *Tetraselmis suecica* was provided daily as a food source (1.0–3.0 × 10^7 cells/L per day).

2.2. Test medium preparation and waterborne exposure

Hg and NMPs working solutions were prepared by diluting the stock solution with 15 psu of ASW. In all experiments, 0.2, 0.4, and 0.8 μg/L of $HgCl_2$ (1/40, 1/20, and 1/10 of 48-h LC_{10} value, respectively; Yoo et al., 2022) and 1 mg/L of each NMPs were used; each concentration was chosen as a sub-lethal concentration and is environmentally relevant in polluted regions (Gao et al., 2014; Kooi et al., 2016). A mixture of Hg and NMPs was prepared at the same concentration as the sole Hg and NMP solutions. Tween 20 (Bio-Rad Inc., Hercules, CA, USA) was added at a final volume of 0.0001 % (v/v) to disperse the PS NMPs in the test medium, and the same concentration of Tween 20 was added to all test media to minimize the effects of the dispersant on the test organism. To adsorb Hg ion on the surface of NMPs, mixture solutions were placed in a shaking incubator at 150 rpm and 25°C for 24 h before use. This duration was selected because most heavy metals, including Hg, exhibit almost maximum adsorption on MPs before 24 h (Hildebrandt et al., 2021). In addition, the Hg and NMP solutions were incubated under the same conditions before use.

For the Hg accumulation and MXR activity assays, Hg and NMPs working solutions were prepared at 0.8 μg/L of $HgCl_2$, 1 mg/L of each NMP (1.46 × 10^{13} particles of 0.05-μm, 1.46 × 10^{10} particles of 0.5-μm, and 8.4 × 10^6 of 6-μm, according to manufacturer's information), and their mixtures. Varying concentrations of 0.2, 0.4, and 0.8 μg/L of $HgCl_2$, 1 mg/L of each NMP, and their mixture were prepared for analysis of transcriptional modulation. After preparing the test medium, adult *D. celebensis* (4-day-old) was exposed to 100 mL of test medium at a density of 1 individual/1 mL in a glass beaker for 48 h without food. All exposure experiments are performed in triplicates for Hg accumulation and MXR activity and in duplicates for gene expression study. Subsequently, *D. celebensis* was pooled in test medium and used for further analysis. For *in vivo* chronic toxicity tests, neonates < 24 h old were individually exposed to 4 mL of $HgCl_2$ (0.8 μg/L), 1 mg/L of each NMP, and their mixture in a 12-well culture plate. A chronic toxicity test was conducted using 12 biological replicates. During chronic exposure, the test medium was renewed every 24 h, newborn neonates were removed, the first reproduction time, total offspring, and lifespan were recorded, and *T. suecica* was provided as a food source (1.0 × 10^7 cells/L per day). All the test vessels were rinsed with 1 % trace metal grade HCl before use.

2.3. Total Hg ion measurement on NMPs and in biota samples

To determine Hg adsorption on NMPs, 200 mL each of the sole-Hg solution and Hg+NMPs mixture were prepared at 10 times the

exposure test (8 μg/L of $HgCl_2$ and 10 mg/L of each NMP) to recover a sufficient amount of NMPs and incubated at the same conditions described in Section 2.2. After incubation, each test solution was filtered using a polyethersulfone (PES) membrane filter (0.03-μm, Sterlitech, Auburn, WA, USA) and freeze-dried before weighing. The NMPs were recovered to > 80 % of nominal concentration (> 1.6 mg). To analyze Hg accumulation in the biota, *D. celebensis* were harvested after 48 h of exposure to sole-Hg and Hg+NMPs mixture, respectively, and rinsed with an ethylenediamine tetraacetic acid (EDTA) solution (25 mM, pH 8.0) and ASW. Subsequently, biota samples in microtubes were digested with ultrapure nitric acid on a hotplate (~120°C) for 24 h. Then, ultrapure hydroperoxide was added into samples after cooling, and heated on a plate at ~120°C for 24 h. The digested samples were diluted and used to analyze the total Hg ion concentrations in the biota. The concentration of total Hg (THg) adsorbed on NMPs and THg accumulated in the biota was measured using a cold vapor atomic fluorescence spectrometer (CVAFS) according to EPA method 1631 (EPA, 2002). The extraction recovery was estimated by extracting a certified reference material (CRM; NIST-2976), as with the sample extraction. The recovery rate was 76.0±3.57 % for plastic samples and 84.9±5.64 % for biota samples. For the filtered solution samples, the CRM recovery (BCR-579) was 111±10.5 %. The method detection limit for THg measurement was 13.2 ng/g dry and 0.17 μg/L in solid and filtered solution samples, respectively. The extraction blank contained approximately 1 % of the measured THg concentration, indicating that the sample was not contaminated during extraction. All experiments were conducted in experimental and technical duplicates.

2.4. Multixenobiotic resistance (MXR) activity assay

MXR activity was measured following the method described by Jeong et al. (2018) with minor modifications. Rhodamine B and calcein AM are substrates for P-gp (ABCB) and MRP (ABCC), thus their high accumulation in the body indicates reduced MXR activity. Accumulation of each fluorescent dye (rhodamine B and calcein AM) following MXR inhibition was confirmed using verapamil and MK-571 as inhibitors of P-gp and MRP, respectively (Figure S1). To investigate MXR activity, after 48 h of single and combined exposure to Hg and NMPs, *D. celebensis* was harvested and washed with ASW. Subsequently, *D. celebensis* was exposed to ASW with 5 μM of rhodamine B or 1 μM of calcein AM for 2 h under dark conditions and rinsed with clean ASW for further analysis. Five individuals were fixed with 4 % formaldehyde solution and analyzed using a fluorescence microscope (Olympus, Tokyo, Japan), while the rest were analyzed using a fluorescence microplate reader. To quantify the fluorescence of each substrate in the body, *D. celebensis* was homogenized in 1 mL of phosphate-buffered saline (PBS) and centrifuged at 13,000 × g for 15 min. Subsequently, the fluorescence in the supernatants was measured using a fluorescence microplate reader (SpectraMax i3x, Molecular Devices, CA, USA) at $Ex_{535\ nm}/Em_{590\ nm}$ for rhodamine B and $Ex_{485\ nm}/Em_{535\ nm}$ for calcein AM to determine the inhibition of ABC transporter activity. All measurements were conducted in triplicate, and fluorescence intensity was normalized based on the total protein content measured using the Bradford assay (Bradford, 1976).

2.5. Total RNA extraction, cDNA synthesis, and quantitative real-time polymerase chain reaction (qRT-PCR)

For transcriptional analysis, *D. celebenesis* was harvested and rinsed with clean ASW after 48 h of exposure to each test medium. Subsequently, total RNA was extracted with TRIZOL® Reagent (Thermo Fisher Scientific Inc., Waltham, MA, USA) following the manufacturer's instructions, and the quality and quantity of total RNA were checked using gel electrophoresis and a NanoDrop8000 spectrophotometer (Thermo Fisher Scientific Inc., Waltham, MA, USA). 500 ng of total RNA was used for cDNA synthesis using the RevertAid First-strand cDNA Synthesis Kit (Thermo Fisher Scientific Inc., USA), and the cDNA was diluted 10-fold with TE buffer for quantitative reverse transcriptase polymerase chain reaction (qRT-PCR). qRT-PCR was conducted using the SYBR master mix (KAPA Bioassay System, USA) with a CFX Connect Thermal Cycler (Bio-Rad Inc., Hercules, CA, USA) according to the following procedures. Briefly, we mixed 5 μL of 2X SYBR mix, 3 μL of diluted cDNA, and 1 μL of each forward and reverse primer listed in Table S2 (Yoo et al., 2024). The mixtures were then incubated at 95 °C for 10 min, and 35 cycles of 95 °C for 15 s and 60 °C for 1 min. The relative gene expression in each group was calculated using the $2^{-\triangle\triangle Ct}$ method (Livak and Schmittgen, 2001) with *elongation factor 1-beta* (*EF1β*) as a reference gene to normalize the Ct value of target genes. All analyses were performed in triplicate, and gene expression patterns were represented by heatmaps using MeV software (version 4.9; Dana-Farber Cancer Institute, Boston, MA, USA).

2.6. Statistical analysis

Statistical analysis was conducted using Sigmaplot version 12.0 (Systat Software Inc., San Jose, CA, USA) and SPSS version 23.0 (SPSS Inc., Chicago, IL, USA), and data were represented as mean ± standard deviation (SD). Before the analysis, the homogeneity of variance was checked using Levene's test ($p > 0.05$). Significant differences in Hg adsorption on NMPs, Hg accumulation in the biota, and transcriptional and enzymatic modulation of ABC transporters between groups were analyzed using one-way analysis of variance (one-way ANOVA), followed by post-hoc analysis using Tukey's HSD test or Dunnett-T3. In all statistical analyses, a *p*-value of less than 0.05 was considered significant.

3. Results

3.1. Hg adsorption on NMPs and accumulation in D. celebensis

The THg concentration adsorbed on the NMPs and accumulated in the biota are presented in Fig. 1. After 24 h of incubation, the Hg adsorption capacity of the NMPs depended on their size (0.05-μm > 0.5-μm > 6-μm). The 0.05-μm PS NPs adsorbed a higher amount of Hg (17.85±0.06 $\mu g/g^{plastics}$) than other sizes (adsorption of Hg on 0.5- and 6-μm MPs: 3.81±0.70, and 2.31±0.43 $\mu g/g^{plastics}$, respectively; Fig. 1**A**). After 48 h exposure to sole-Hg, THg concentration in biota was 6.04 ±0.09 $\mu g/g^{biota}$, which was increased by co-exposure to 0.05-μm PS NP (21.03±2.04 $\mu g/g^{biota}$) but was decreased by 6-μm MPs (3.76±0.29 $\mu g/g^{biota}$) (Fig. 1**B**).

3.2. Effects of Hg, NMPs, and their mixture on MXR activity of D. celebensis

MXR inhibition by *D. celebensis* was analyzed by measuring the fluorescence of rhodamine B (a substrate of P-gp) and calcein AM (a substrate of MRP). After exposure to NMP alone, the fluorescence intensity of rhodamine B and calcein AM was negatively modulated depending on the size of the NMPs (Fig. 2).

Among NMPs, 0.05- and 0.5-μm PS beads induced inhibition of both transporters (increased fluorescent intensity of rhodamine B and calcein AM), with the highest inhibition observed in the 0.05-μm exposure group. In contrast, 6-μm MP exposure did not affect MXR activity. In the case of Hg exposure, in the single Hg-exposed group, significantly increased MRP activity was observed (decreased fluorescence of calcein AM). However, the activity of P-gp did not change by Hg exposure. The activity of both transporters in the Hg-exposed group was inhibited by 0.05- and 0.5-μm PS co-exposure, with the highest inhibition observed in the 0.05-μm exposure group (Fig. 3).

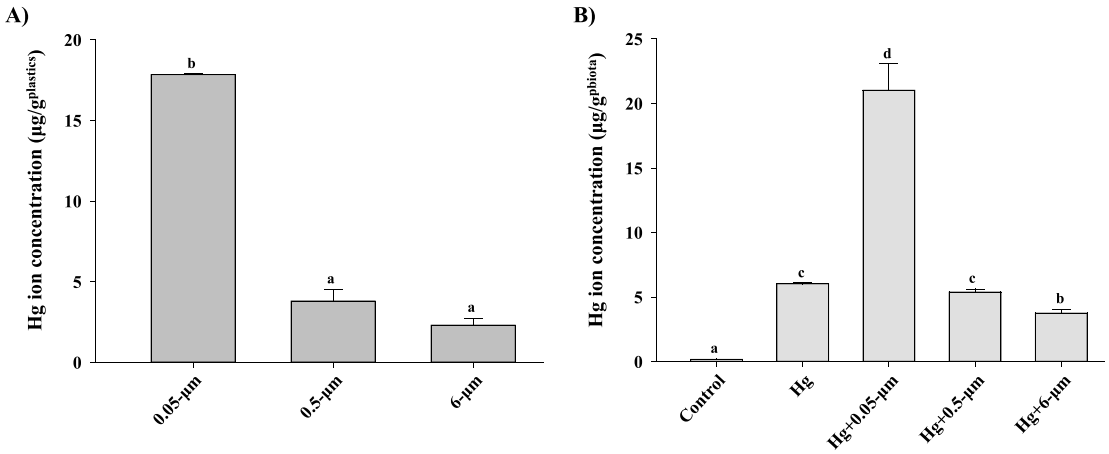

Fig. 1. Hg concentration on A) surface of nano- and microplastics (NMPs) after 24 h incubation (10 mg/L of NMPs and 8 μg/L of $HgCl_2$) and in *Diaphanosoma celebensis* after 48 h exposure to single Hg (0.8 μg/L of $HgCl_2$) and combined exposure to Hg (0.8 μg/L of $HgCl_2$) and NMPs (1 mg/L). Different letters indicate significant differences among exposed groups (one-way ANOVA, $p < 0.05$). Data are presented as mean ± standard error of the mean (n = 2).

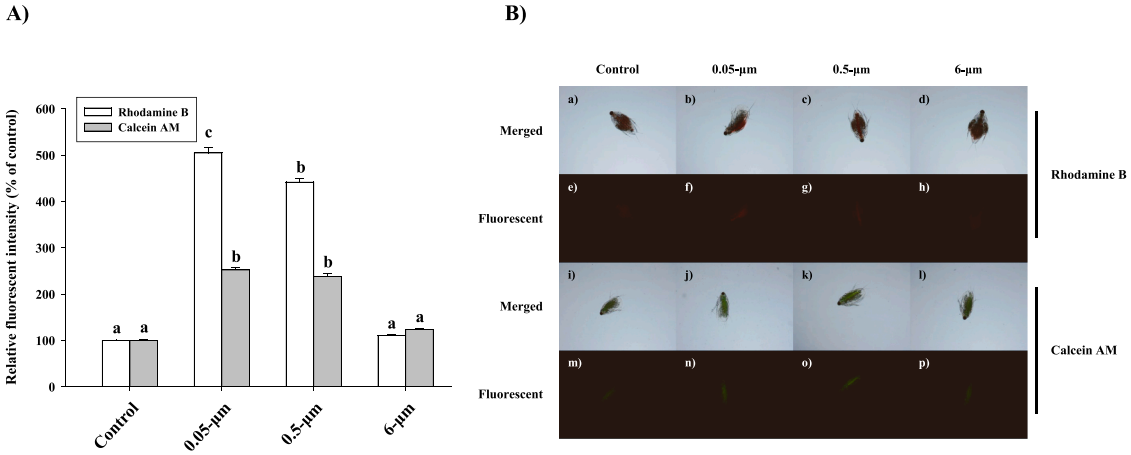

Fig. 2. The fluorescent intensity of accumulated rhodamine B and calcein AM in the *Diaphanosoma celebensis* after 1 mg/L of NMPs (0.05-, 0.5-, and 6-μm) exposure for 48-h. A) the relative fluorescent intensity, B) fluorescence images of each substrate. Different letters indicate significant differences within the exposure group (one-way ANOVA, $p < 0.05$). Data are presented as mean ± standard deviation of the mean (n = 3).

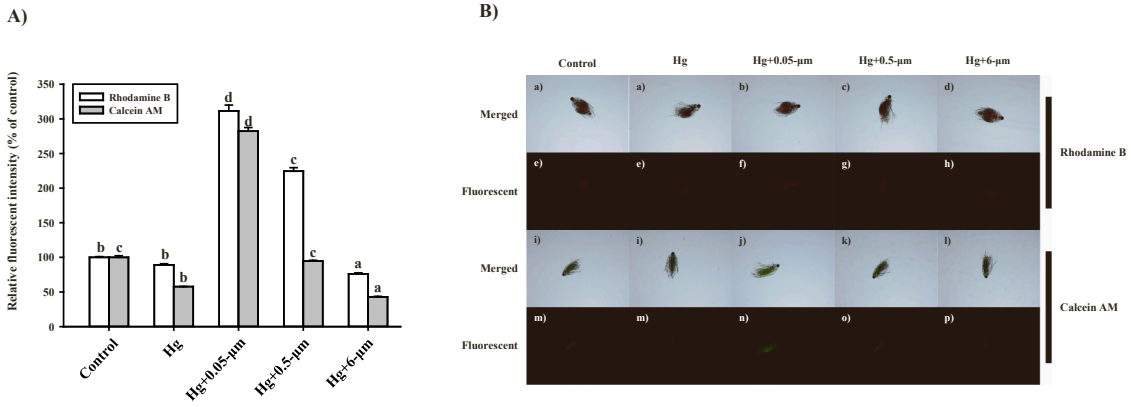

Fig. 3. The fluorescent intensity of accumulated rhodamine B and calcein AM in the *Diaphanosoma celebensis* after sole-Hg (0.8 μg/L) and Hg with 1 mg/L of NMPs (0.05-, 0.5-, and 6-μm) exposure for 48-h. A) The relative fluorescence intensity, B) fluorescence images of each substrate. Different letters indicate significant differences within the exposure group (one-way ANOVA, $p < 0.05$). Data are presented as mean ± standard deviation of the mean (n = 3).

3.3. Transcriptional modulation of MXR-related genes

The transcriptional modulation of 11 ABC transporter genes (six *ABCBs* and five *ABCCs*) in *D. celebensis* exposed to single and combined exposure to Hg and NMPs was analyzed (Fig. 4, Table S3). After single-Hg exposure, the expression of *ABCB1–1* and *ABCC1–1* significantly increased (1.52- and 1.61-fold, respectively) compared to that in the control group after 0.8 μg/L of $HgCl_2$ exposure, but expression of *ABCC9*

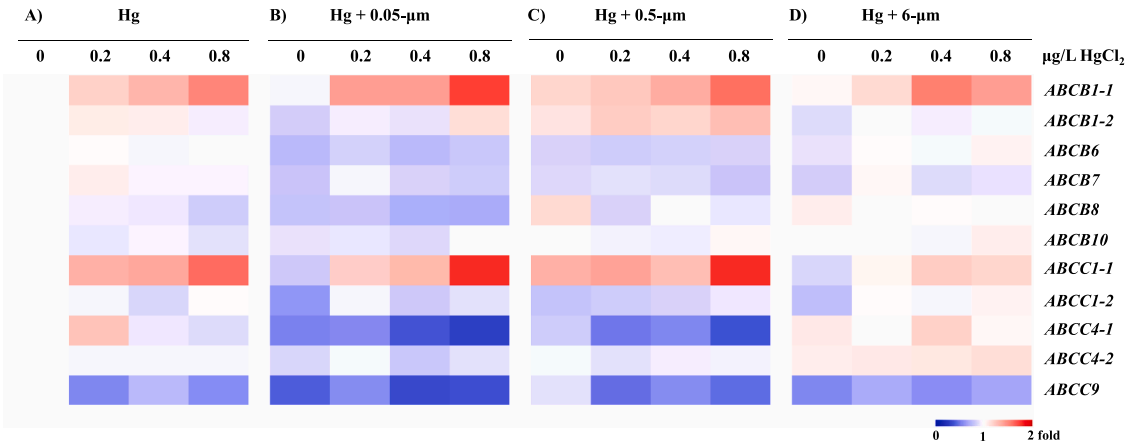

Fig. 4. Transcriptional modulation patterns of ABCB and ABCC subfamily genes in *Diaphanosoma celebensis* after sole-Hg (0, 0.2, 0.4, and 0.8 μg/L) and Hg with 1 mg/L of NMPs (0.05-, 0.5-, and 6-μm) exposure for 48-h. A) Hg, B) Hg+0.05-μm PS beads, C) Hg+0.5-μm PS beads, and D) Hg+6-μm PS beads.

was decreased (0.54- and 0.57-fold after 0.2 and 0.8 μg/L of $HgCl_2$ exposure, respectively; Fig. 4**A**). After exposure to 0.05-μm PS, most of the ABC transporter genes were significantly down-regulated (< 0.80-fold compared to the control group). In addition, co-exposure to 0.05-μm PS+Hg further increased the expression of genes that were increased by Hg exposure, especially *ABCB1–1* and *ABCC1–1*, at the same Hg concentration, and vice versa (Fig. 4**B**). The 0.5-μm PS co-exposure also further increased the expression of *ABCC1–1* (1.79-fold compared to that of the control group after 0.8 μg/L of $HgCl_2$ exposure) and further decreased the expression of *ABCC4–1* and *ABCC9* (0.37- and 0.46-fold compared to that of the control group after 0.8 μg/L of $HgCl_2$, respectively; Fig. 4**C**). In contrast, 6-μm PS co-exposure alleviated the gene

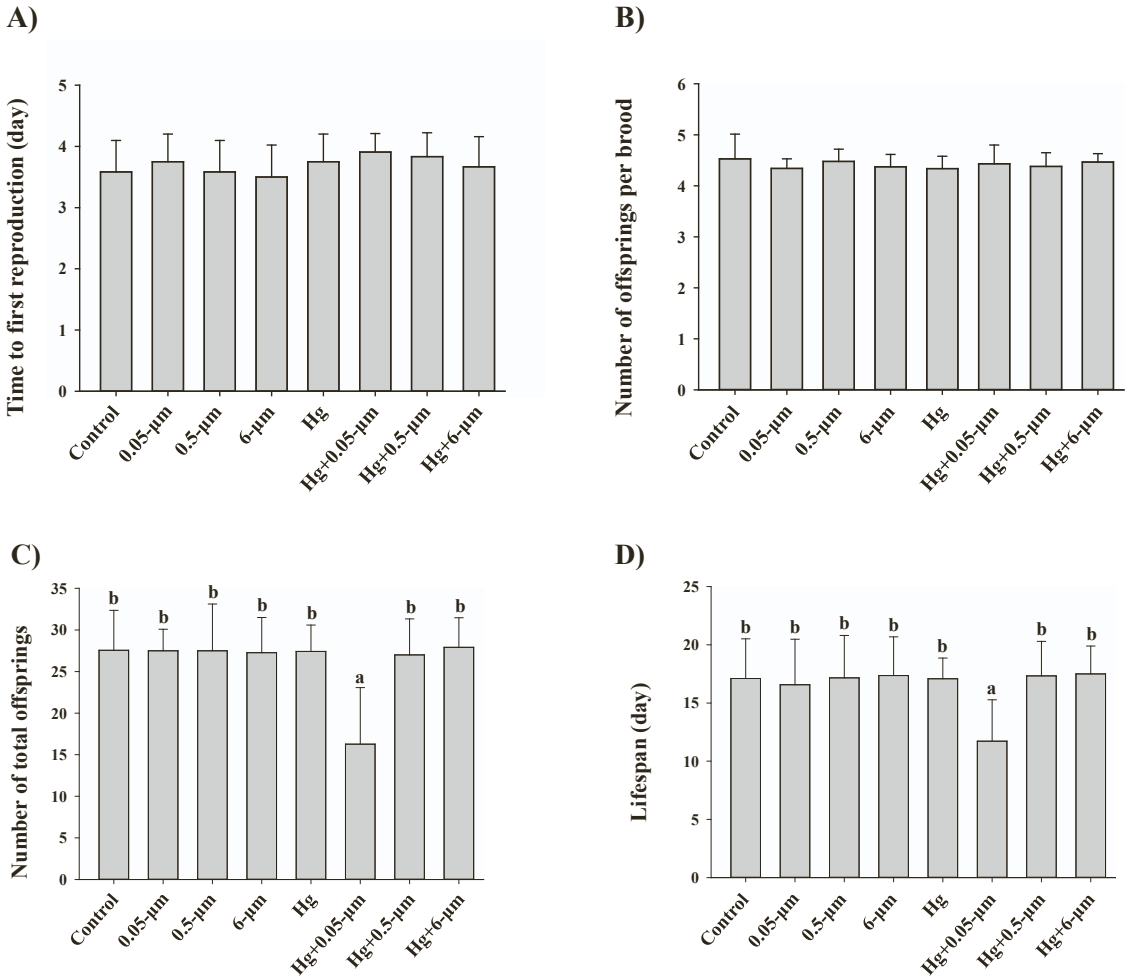

Fig. 5. The chronic effects of single and combined exposure to Hg (0.8 μg/L) and NMPs (0.05-, 0.5-, and 6-μm; 1 mg/L) on A) time to first reproduction, B) number of offspring per brood, C) number of total offspring, and D) lifespan of *Diaphanosoma celebensis*. Different letters indicate significant differences within the exposure group (one-way ANOVA, $p < 0.05$). Data are presented as mean ± standard deviation of the mean (n = 12).

modulation affected by Hg at the same concentrations (Fig. 4**D**).

3.4. Chronic effects of Hg, NMPs, and their mixture on reproduction in D. celebensis

After chronic exposure to PS NMPs, Hg, or their mixture, there were no significant differences in the first reproduction time or number of offspring per brood in all groups (Fig. 5**A** and **B**). The number of total offspring was not significantly different in groups exposed to single NMPs, Hg, and the mixture of Hg with 0.5- or 6-μm PS (Hg+0.5-μm and Hg+6-μm). However, Hg+0.05-μm exposure significantly reduced the number of total offspring (Fig. 5**C**). Lifespan was also significantly reduced only in the group co-exposed to Hg and the 0.05-μm PS NPs (Fig. 5**D**).

4. Discussion

NMPs can adsorb various contaminants on their surfaces via both physisorption and chemisorption mechanisms such as van der Waals forces, π–π bond, electrostatic, and hydrogen bond interactions (Agboola and Benson, 2021), which can depend on properties of MPs and/or chemicals (Zhao et al., 2020). Previous studies reported the adsorption of heavy metals, including arsenic, cadmium, lead, and aluminum on marine MPs collected from coastal regions (Liu et al., 2022), and Hg adsorption on MPs collected from beaches (20.4 $\mu g/g^{plastics}$; Turner et al., 2019) and seawater (170 $ng/g^{plastics}$; Bowman et al., 2021). In this study, we confirmed the adsorption of the Hg^{2+} ion on NMPs, and the 0.05-μm NPs showed the highest adsorption capacity. Similarly, Xie et al. (2022) confirmed the concentration-dependent adsorption of Hg on NPs (0.05-μm, PS) after 48 h incubation of 0–10 μg/L of Hg (added as $HgCl_2$) with 23 μg/L of NPs under laboratory conditions and observed a high equilibrium adsorption of Hg (82.33 $mg/g^{plastics}$) after incubation of 10 μg/L of Hg with NPs. Thus, our results suggest that NMPs have a high affinity for Hg and can act as a carrier of Hg to marine biota and that the smaller the plastics are, the more Hg they can adsorb, which may be due to their high surface/volume ratio. Previous studies have reported that co-exposure to NMPs can affect the bioaccumulation of heavy metals, including Hg, in aquatic organisms. For example, co-exposure to 1–5–μm MPs increased Hg bioaccumulation in the gills and liver of European seabass *Dicenthrarchus labrax* (Barboza et al., 2018) and bioaccumulation of copper (Cu) in zebrafish exposed to $CuSO_4$ was increased by co-exposure to 0.1 and 20 μm PS NMPs (Qiao et al., 2019). Consistent with the previous studies, Hg accumulation in *D. celebensis* exposed to $HgCl_2$ (6.04 $\mu g/g^{biota}$) was increased by co-exposure to the 0.05-μm NPs (21.03 $\mu g/g^{biota}$). Thus, our results imply that NPs can transfer Hg into the biota as carriers, thereby increasing Hg accumulation. However, Xie et al. (2022) reported that although Hg accumulation in the marine copepod *T. japonicus* was increased by co-exposure to NPs, Hg accumulation in both groups exposed to sole-Hg and Hg+NPs was not significantly different after 24 h of depuration in clean media. Thus, the authors suggested that PS NPs could transport Hg into the marine copepod *T. japonicus*, but that the NPs did not increase the bioaccumulation of Hg. Nevertheless, because organisms do not undergo depuration and are continuously exposed to pollutants in the natural marine environment, the increase in Hg accumulation due to NPs should not be disregarded. Although co-exposure to NPs increased Hg accumulation in *D. celebensis*, the effects of NMPs on Hg accumulation depended on their size; the group exposed to Hg+0.5-μm showed no significant differences with the group exposed to sole-Hg, and co-exposure to 6-μm MPs reduced Hg accumulation in *D. celebensis*, which suggests that size of NMPs is an important factor for toxicological interaction with Hg. Some previous studies also reported reduced bioaccumulation of Hg by co-exposure to MPs in bivalve *C. fluminea* (size of MP was 1–5-μm; Oliveira et al., 2018) and manila clam *R. philippinarum* (size of MP was 10–45-μm; Sikdokur et al., 2020). According to these authors, the reduced Hg accumulation in the biota may be due to the decreased bioavailability of Hg in the test media by the adsorption of Hg on MPs. Similarly, after 24 h of incubation of the Hg+NMPs mixture in this study, there was a decrease in the Hg concentration in the test media (~36 % of the initial concentration; data not shown). Thus, the decrease of Hg accumulation in *D. celebensis* by the 6-μm MP co-exposure in this study is possibly associated with the reduced bioavailability of Hg in the test media by MPs. However, given that the vector effects of NMPs are closely related to the adsorption and desorption kinetics of pollutants (Amelia et al., 2021; Xie et al., 2022), further studies on the desorption of Hg adsorbed on NMPs under *in vivo* conditions should be conducted to better understand the size-dependent vector effects of NMPs on Hg accumulation in biota.

On the other hand, co-exposure to NMPs can affect the accumulation of pollutants in biota not only by adsorbing and transferring chemicals to biota but also by altering MXR as a cellular defense system. The smaller the size of NMPs, the higher the disruption of MXR (Franzellitti et al., 2019; Jeong et al., 2018). Thus, impairment of efflux activity of Hg may be one of the reasons for increased Hg accumulation by the 0.05-μm NPs, together with the transfer of high concentration of Hg to biota by NPs as a carrier. Because P-gp (ABCB subfamily) and MRP (ABCC subfamily) are phase III detoxification enzymes that play important roles in the efflux of pollutants, including heavy metals (Bridges and Zalups., 2017; Jeong et al., 2017), we investigated the single and combined effects of Hg and NMPs on P-gp and/or MRP-mediated MXR in *D. celebensis*. In this study, the accumulation of both rhodamine B and calcein AM, fluorescent substrates of P-gp and MRP, respectively, was significantly increased in the groups exposed to the 0.05- and 0.5-μm PS, which suggests that exposure to NMPs can disturb MXR activity in *D. celebensis*. Similarly, Jeong et al. (2018) reported a disruption of MXR in rotifer *Brachionus koreanus* after exposure to 0.05- and 0.5-μm PS NMPs, and suggested an increase in oxidative stress and disruption of lipid membranes upon NMPs exposure as the reason, which is consistent with our previous findings of size-dependent toxicity of NMPs on oxidative stress and increased lipid peroxidation in *D. celebensis* following 0.05-μm PS exposure (Yoo et al., 2021, 2022). Contrary to NMP exposure alone, Hg exposure reduced the accumulation of calcein AM, suggesting increased MRP activity, which well matched with the up-regulation of *ABCC1–1*. The fluorescence of rhodamine B was not significantly affected, although *ABCB1–1* was up-regulated upon exposure to Hg. In various animals, including aquatic organisms, intracellular Hg^{2+} is conjugated with thiol-containing molecules and excreted via both amino acid transporters and MRPs, but it remains unclear whether P-gp is involved in Hg^{2+} excretion (Bridges and Zalups, 2017; Luckenbach et al., 2014). Similar to this study, our previous study showed that organic Hg exposure also increased the efflux activity of MRPs but not P-gp (Yoo et al., 2024). Campos et al. (2014) reported that Hg exposure decreased the accumulation of calcein AM in the freshwater water flea *Daphnia magna* with up-regulation of *ABCC*, but not rhodamine B. These results suggested that MRPs (ABCC), rather than P-gp (ABCB), play an important role in Hg efflux in this species. However, the MXR activity of ABC transporters in *D. celebensis* exposed to Hg was altered by co-exposure to NMP. Especially, in contrast to sole-Hg, the Hg+0.05-μm exposure increased accumulation of both rhodamine B and calcein AM, and the 0.05-μm and Hg+0.05-μm exposure down-regulated most of the ABC transporter genes except for *ABCB1–1* and *ABCC1–1*, which were up-regulated by sole-Hg exposure (Figs. 3 and 4). The increased accumulation of both substrates of P-gp and MRP and decreased expression of *ABCBs* and *ABCCs* suggests disturbed MXR activity, which might be due to cellular membrane disruption caused by the 0.05-μm and Hg+0.05-μm exposure (Jeong et al., 2018), and the highest Hg accumulation in the group exposed to Hg+0.05-μm is likely to be closely related to the disruption of MXR. The *in vivo* toxicity test showed synergistic toxicity between Hg and 0.05-μm NPs. The number of total offspring and lifespan of *D. celebensis* were significantly decreased only in the group exposed to Hg+0.05-μm, which was consistent with a previous study reported synergistic chronic toxicity of Hg and NPs on Hg

accumulation in *T. japonicus* and their survival rate and fecundity (Xie et al., 2023). Our previous study confirmed that co-exposure to 0.05-μm NPs increased Hg-induced oxidative stress and mortality in *D. celebensis* (Yoo et al., 2022). Given the results of Hg accumulation and MXR activity assays, synergistic *in vivo* toxicity between 0.05-μm NPs and Hg may be due to enhanced Hg-induced toxicity, such as oxidative stress and cytotoxicity (Yoo et al., 2022), due to increased Hg accumulation by NPs. However, time to first reproduction and number of offspring per brood were not significantly different compared to that of the control group, which implies that co-exposure of Hg and NPs does not seem to directly affect reproduction (such as delayed reproduction and/or decreased fertility) of *D. celebensis* but may cause potential reproductive toxicity by reducing lifespan. Taken together, our results suggest that NPs can increase Hg accumulation not only by acting as a carrier to transfer Hg but also by disrupting MXR, consequently leading to increased toxicity of Hg even at low Hg concentration.

5. Conclusion

Ocean plastic pollution, especially NMPs pollution, and Hg pollution are considered major environmental issues. Because NMPs co-exist with various pollutants and can interact with them, the toxicological interactions between NMPs and pollutants, including Hg, should be understood. According to our findings, PS NMPs can act as potential carriers of Hg and/or inhibitors of MXR in marine zooplankton, altering Hg accumulation in biota. However, the Hg adsorption and MXR disruption by NMPs depend on their size. In particular, NPs had the highest Hg adsorption capacity and inhibition of MXR, and increased the accumulation and toxicity of Hg in the biota, suggesting a synergistic interaction between NPs and Hg. This study provides information on the toxicological interactions between NMPs and Hg and will be helpful for a better understanding of the interactions between plastics and other pollutants in the ocean. However, because toxicological interaction between NMPs and ambient pollutants can vary depending on various factors, such as functional groups, surface roughness, shape, and polymer type of NMPs, and/or the hydrophobicity of chemicals, further studies on toxicological interactions with different plastics and chemicals should be conducted.

Funding

This research was supported by the National Research Foundation of Korea (NRF) grant funded by the Korean government (MSIT) (No. 2020R1F1A1069736) and the "Risk assessment to prepare standards for protecting marine ecosystem" of the Korea Institute of Marine Science & Technology Promotion (KIMST) funded by the Ministry of Oceans and Fisheries (KIMST-20220383).

CRediT authorship contribution statement

Kyun-Woo Lee: Writing – review & editing, Resources. **Seunghee Han:** Writing – review & editing, Methodology. **Young-Mi Lee:** Writing – review & editing, Supervision, Funding acquisition, Conceptualization. **Youn-Ha Lee:** Resources, Methodology. **Je-Won Yoo:** Writing – original draft, Investigation, Formal analysis. **Jihee Kim:** Methodology.

Declaration of Competing Interest

The authors declare that they have no known competing financial interests or personal relationships that could have appeared to influence the work reported in this paper.

Data Availability

Data will be made available on request.

Appendix A. Supporting information

Supplementary data associated with this article can be found in the online version at doi:10.1016/j.ecoenv.2024.117131.

References

Agboola, O.D., Benson, N.U., 2021. Physisorption and chemisorption mechanisms influencing micro (nano) plastics-organic chemical contaminants interactions: a review. Front. Environ. Sci. 9, 167. https://doi.org/10.3389/fenvs.2021.678574.

Ajith, N., Arumugam, S., Parthasarathy, S., et al., 2020. Global distribution of microplastics and its impact on marine environment—a review. Environ. Sci. Pollut. 27, 25970–25986. https://doi.org/10.1007/s11356-020-09015-5.

Amelia, T.S.M., Khalik, W.M.A.W.M., Ong, M.C., et al., 2021. Marine microplastics as vectors of major ocean pollutants and its hazards to the marine ecosystem and humans. Prog. Earth Planet. Sci. 8 (1), 1–26. https://doi.org/10.1186/s40645-020-00405-4.

Barboza, L.G.A., Vieira, L.R., Branco, V., et al., 2018. Microplastics increase mercury bioconcentration in gills and bioaccumulation in the liver, and cause oxidative stress and damage in *Dicentrarchus labrax* juveniles. Sci. Rep. 8 (1), 15655. https://doi.org/10.1038/s41598-018-34125-z.

Bhagat, J., Nishimura, N., Shimada, Y., 2021. Toxicological interactions of microplastics/nanoplastics and environmental contaminants: current knowledge and future perspectives. J. Hazard. Mat. 405, 123913. https://doi.org/10.1016/j.jhazmat.2020.123913.

Birch, Q.T., Potter, P.M., Pinto, P.X., et al., 2020. Sources, transport, measurement and impact of nano and microplastics in urban watersheds. Rev. Environ. Sci. Biotechnol. 19, 275–336. https://doi.org/10.1007/s11157-020-09529-x.

Bowman, K.L., Lamborg, C.H., Agather, A.M., et al., 2021. The role of plastic debris in the biogeochemical cycle of mercury in Lake Erie and San Francisco Bay. Mar. Pollut. Bull. 171, 112768. https://doi.org/10.1016/j.marpolbul.2021.112768.

Bradford, M.M., 1976. A rapid and sensitive method for the quantitation of microgram quantities of protein utilizing the principle of protein-dye binding. Anal. Biochem. 72 (1-2), 248–254. https://doi.org/10.1016/0003-2697(76)90527-3.

Brennecke, D., Duarte, B., Paiva, F., et al., 2016. Microplastics as vector for heavy metal contamination from the marine environment. Estuar. Coast. Shelf Sci. 178, 189–195. https://doi.org/10.1016/j.ecss.2015.12.003.

Bridges, C.C., Zalups, R.K., 2017. Mechanisms involved in the transport of mercuric ions in target tissues. Arch. Toxicol. 91 (1), 63–81. https://doi.org/10.1007/s00204-016-1803-y.

Cai, M., He, H., Liu, M., et al., 2018. Lost but can't be neglected: huge quantities of small microplastics hide in the South China Sea. Sci. Total Environ. 633, 1206–1216. https://doi.org/10.1016/j.scitotenv.2018.03.197.

Campos, B., Altenburger, R., Gómez, C., et al., 2014. First evidence for toxic defense based on the multixenobiotic resistance (MXR) mechanism in *Daphnia magna*. Aquat. Toxicol. 148, 139–151. https://doi.org/10.1016/j.aquatox.2014.01.001.

Cho, H., Jeong, C.B., Lee, Y.M., 2022. Modulation of ecdysteroid and juvenile hormone signaling pathways by bisphenol analogues and polystyrene beads in the brackish water flea *Diaphanosoma celebensis*. Comp. Biochem. Physiol. C. 262, 109462. https://doi.org/10.1016/j.cbpc.2022.109462.

DeMott, W.R., 1986. The role of taste in food selection by freshwater zooplankton. Oecologia 69, 334–340. https://doi.org/10.1007/BF00377053.

El-Awady, R., Saleh, E., Hashim, A., et al., 2017. The role of eukaryotic and prokaryotic ABC transporter family in failure of chemotherapy. Front. Pharmacol. 7, 535. https://doi.org/10.3389/fphar.2016.00535.

Eo, S., Hong, S.H., Song, Y.K., et al., 2018. Abundance, composition, and distribution of microplastics larger than 20 μm in sand beaches of South Korea. Environ. Pollut. 238, 894–902. https://doi.org/10.1016/j.envpol.2018.03.096.

EPA, U., 2002. Method 1631. Revision E: Mercury in Water by Oxidation, Purge and Trap, and Cold Vapor Atomic Fluorescence Spectrometry. US Environmental Protection Agency, Washington, D.C.

Franzellitti, S., Capolupo, M., Wathsala, R.H., et al., 2019. The multixenobiotic resistance system as a possible protective response triggered by microplastic ingestion in mediterranean mussels (*Mytilus galloprovincialis*): larvae and adult stages. Comp. Biochem. Physiol. C. 219, 50–58. https://doi.org/10.1016/j.cbpc.2019.02.005.

Gao, X., Zhou, F., Chen, C.T.A., 2014. Pollution status of the Bohai sea: an overview of the environmental quality assessment related trace metals. Environ. Int. 62, 12–30. https://doi.org/10.1016/j.envint.2013.09.019.

Gworek, B., Bemowska-Kałabun, O., Kijeńska, M., et al., 2016. Mercury in marine and oceanic waters—a review. Water Air Soil Pollut. 227 (10), 371. https://doi.org/10.1007/s11270-016-3060-3.

Hildebrandt, L., Nack, F.L., Zimmermann, T., et al., 2021. Microplastics as a Trojan horse for trace metals. J. Hazard. Mater. Lett. 2, 100035. https://doi.org/10.1016/j.hazl.2021.100035.

Jeon, M.J., Yoo, J.W., Lee, K.W., et al., 2023. Microplastics disrupt energy metabolism in the brackish water flea diaphanosoma celebensis. Comp. Biochem. Physiol. C. 271, 109680. https://doi.org/10.1016/j.cbpc.2023.109680.

Jeong, C.B., Kang, H.M., Lee, Y.H., et al., 2018. Nanoplastic ingestion enhances toxicity of persistent organic pollutants (POPs) in the monogonont rotifer *Brachionus koreanus* via multixenobiotic resistance (MXR) disruption. Environ. Sci. Technol. 52 (19), 11411–11418. https://doi.org/10.1021/acs.est.8b03211.

Jeong, C.B., Kim, H.S., Kang, H.M., et al., 2017. Genome-wide identification of ATP-binding cassette (ABC) transporters and conservation of their xenobiotic transporter

function in the monogonont rotifer (*Brachionus koreanus*). Comp. Biochem. Physiol. D. 21, 17–26. https://doi.org/10.1016/j.cbd.2016.10.003.
Kik, K., Bukowska, B., Sicińska, P., 2020. Polystyrene nanoparticles: sources, occurrence in the environment, distribution in tissues, accumulation. Toxic. Var. Org. Environ. Pollut. 262, 114297. https://doi.org/10.1016/j.aquatox.2021.105821.
Kooi, M., Reisser, J., Slat, B., et al., 2016. The effect of particle properties on the depth profile of buoyant plastics in the ocean. Sci. Rep. 6 (1), 33882. https://doi.org/10.1038/srep33882.
Liu, Y., Zhang, K., Xu, S., et al., 2022. Heavy metals in the "plastisphere" of marine microplastics: adsorption mechanisms and composite risk. Gondwana Res 108, 171–180. https://doi.org/10.1016/j.gr.2021.06.017.
Livak, K.J., Schmittgen, T.D., 2001. Analysis of relative gene expression data using real-time quantitative PCR and the $2^{-\Delta\Delta CT}$ method. methods 25 (4), 402–408. https://doi.org/10.1006/meth.2001.1262.
Luckenbach, T., Fischer, S., Sturm, A., 2014. Current advances on ABC drug transporters in fish. Comp. Biochem. Physiol. C. 165, 28–52. https://doi.org/10.1016/j.cbpc.2014.05.002.
Oliveira, P., Barboza, L.G.A., Branco, V., et al., 2018. Effects of microplastics and mercury in the freshwater bivalve *Corbicula fluminea* (Müller, 1774): filtration rate, biochemical biomarkers and mercury bioconcentration. Ecotoxicol. Environ. Saf. 164, 155–163. https://doi.org/10.1016/j.ecoenv.2018.07.062.
PlasticsEurope, 2023. Plastics – The fast facts 2023. ⟨https://plasticseurope.org/knowledge-hub/plastics-the-fast-facts-2023/⟩. (Accessed 21 April 2024).
Qiao, R., Lu, K., Deng, Y., et al., 2019. Combined effects of polystyrene microplastics and natural organic matter on the accumulation and toxicity of copper in zebrafish. Sci. Total Environ. 682, 128–137. https://doi.org/10.1016/j.scitotenv.2019.05.163.
Sikdokur, E., Belivermiş, M., Sezer, N., et al., 2020. Effects of microplastics and mercury on manila clam *Ruditapes philippinarum*: feeding rate, immunomodulation, histopathology and oxidative stress. Environ. Pollut. 262, 114247. https://doi.org/10.1016/j.envpol.2020.114247.
Turner, A., Wallerstein, C., Arnold, R., 2019. Identification, origin and characteristics of bio-bead microplastics from beaches in western Europe. Sci. Total Environ. 664, 938–947. https://doi.org/10.1016/j.scitotenv.2019.01.281.
Vasiliou, V., Vasiliou, K., Nebert, D.W., 2009. Human ATP-binding cassette (ABC) transporter family. Hum. Genom. 3 (3), 1–10. https://doi.org/10.1186/1479-7364-3-3-281.
Xie, D., Wei, H., Lee, J.S., et al., 2022. Mercury can be transported into marine copepod by polystyrene nanoplastics but is not bioaccumulated: an increased risk? Environ. Pollut. 303, 119170. https://doi.org/10.1016/j.envpol.2022.119170.
Xie, D., Zhang, H., Wei, H., et al., 2023. Nanoplastics potentiate mercury toxicity in a marine copepod under multigenerational exposure. Aquat. Toxicol. 258, 106497. https://doi.org/10.1016/j.aquatox.2023.106497.
Yan, H., Li, Q., Yuan, Z., et al., 2019. Research progress of mercury bioaccumulation in the aquatic food chain, China: a review. Bull. Environ. Contam. Toxicol. 102, 612–620. https://doi.org/10.1007/s00128-019-02629-7.
Yoo, J.W., Cho, H., Jeon, M., Jeong, C.B., Jung, J.H., Lee, Y.M., 2021. Effects of polystyrene in the brackish water flea Diaphanosoma celebensis: size-dependent acute toxicity, ingestion, egestion, and antioxidant response. Aquat. Toxicol. 235, 105821. https://doi.org/10.1016/j.aquatox.2021.105821.
Yoo, J.W., Choi, T.J., Park, J.S., et al., 2023. Pathway-dependent toxic interaction between polystyrene microbeads and methylmercury on the brackish water flea *Diaphanosoma celebensis*: based on mercury bioaccumulation, cytotoxicity, and transcriptomic analysis. J. Hazard. Mat. 459, 132055. https://doi.org/10.1016/j.jhazmat.2023.132055.
Yoo, J.W., Jeon, M., Lee, K.W., et al., 2022. The single and combined effects of mercury and polystyrene plastic beads on antioxidant-related systems in the brackish water flea: toxicological interaction depending on mercury species and plastic bead size. Aquat. Toxicol. 252, 106325. https://doi.org/10.1016/j.aquatox.2022.106325.
Yoo, J.W., Lee, Y.H., Cho, S., et al., 2024. Combined effects of microplastics and methylmercury on the activity of ATP-binding cassette (ABC) transporter in the brackish water flea *Diaphanosoma celebensis*. Toxicol. Environ. Health Sci. https://doi.org/10.1007/s13530-023-00201-9.
Zhao, L., Rong, L., Xu, J., et al., 2020. Sorption of five organic compounds by polar and nonpolar microplastics. Chemosphere 257, 127206. https://doi.org/10.1016/j.chemosphere.2020.127206.